ELSEVIER

Chemical Engineering Journal 120 (2006) 139–147

Chemical Engineering Journal

www.elsevier.com/locate/cej

Mathematic modeling of the process of production of nanofibrous carbon from methane in an isothermal reactor with a fixed bed of the Ni–Al_2O_3 catalyst

Sergei G. Zavarukhin [a], Gennady G. Kuvshinov [b,*]

[a] *Boreskov Institute of Catalysis, Pr. Akad. Lavrentieva, 5, Novosibirsk 630090, Russia*
[b] *Novosibirsk State Technical University, Pr. K. Marx, 20, Novosibirsk 630092, Russia*

Received 9 March 2005; received in revised form 27 February 2006; accepted 8 March 2006

Abstract

The process of synthesis of nanofibrous carbon from methane achieved in an isothermal plug flow reactor with a fixed bed of catalyst 90 wt.% Ni–Al_2O_3 is considered. It is shown that the equations allow a solution in the form of a progressive wave of deactivation that moves at a constant rate and has a stationary profile. Analytic dependencies are obtained to calculate the wave rate and carbon content in the deactivated catalyst. The process parameters are calculated at 823 K and specific methane consumption 120 l/h g. The process parameters are compared for two types of reactors operating at identical conditions: a plug flow reactor with the fixed catalyst bed and a reactor with perfect mixing of catalyst particles and gas. The specific carbon yield is shown to be higher in the latter.

Keywords: Nanofibrous carbon; Filamentous carbon; Methane decomposition; Ni–Al_2O_3 catalyst; Reactor; Fixed catalyst bed; Ideal gas plugging

1. Introduction

Nanofibrous carbon (NFC) falls into a new class of graphite-like carbon materials synthesized by gas phase decomposition of hydrocarbons or disproportionation of CO in the presence of VIII group metal containing catalysts [1–4]. Depending on the catalysts used, gas mixture compositions and temperature, carbon fibers of three modifications can be produced. These are: multilayer carbon nanotubes (basal planes are deformed into nested cylinders in parallel to the fiber axis), fibers with basal planes perpendicular to the fiber axis, and fibers with planes deformed into nested cones at an angle to the fiber axis. The characteristic size of the catalytically synthesized carbon nanofibers is 10–150 nm depending on the synthetic conditions. Results of numerous studies on properties of the nanofibers carbon materials [2,3,5,6] indicate their numerous application areas including unique sorbents [7], catalysts [8], catalyst supports [9,10], biologically active substances [11], electrodes, fillers in electroconductive plastics and dyes etc.

Typical sites of growth of the carbon nanofibers during the catalytic decomposition of carbon-containing gases are nanoparticles of VIII group metals or of alloys containing these metals. Fig. 1 shows an electron micrograph of a nickel nanoparticle at such a center with a carbon fiber growing thereon [12]. The mechanism of the formation of nanofibrous carbon includes decomposition of hydrocarbons on one type faces of the nanoparticle to produce carbon, dissolution of the carbon in the particle, diffusion of the carbon to another type faces where the carbon nanofibers of a certain structure are released.

In the process of nanofibrous carbon formation, the catalyst is deactivated thus restricting the quantity of carbon produced per unit mass of the catalyst and, consequently, the product purity. In order to enhance the specific (per catalyst unit mass) yield of carbon, the process is normally conducted until the catalyst is fully deactivated. The same target can be achieved by improving the catalyst and optimizing the conditions of NFC synthesis.

Reactors of various types are used in laboratories for synthesis and characterization of NFC. These are tubes with catalyst baskets loaded in them [2,3,13,14], fixed bed reactors [15–19], stirred reactors [20], fluidized bed reactors [3,21–25]. In large-scale NFC production, fluidized bed reactors and stirred reactors are most practiced because of the necessity to stir the materials

* Corresponding author. Fax: +7 3833 460801.
E-mail address: tpa@mail.fam.nstu.ru (G.G. Kuvshinov).

1385-8947/$ – see front matter © 2006 Elsevier B.V. All rights reserved.
doi:10.1016/j.cej.2006.03.004

Nomenclature

a	relative catalyst activity
c	specific carbon content of the catalyst (g/g)
c_m	maximal specific carbon content on the catalyst (g/g)
c_{av}	averaged carbon content on the catalyst (g/g)
G_c	specific carbon yield (g/g), ($=m_c/m_0$)
i	node number along τ
j	node number along z
J_c	flux of carbon in methane feedstock (g/h)
h_z	step of grid along z
h_τ	step of grid along τ
k	temperature dependent coefficient (g/h g bar)
k_a	temperature dependent coefficient (h)
k_H	temperature dependent coefficient (bar $^{-0.5}$)
K_p	equilibrium constant (bar)
m	catalyst mass between the inlet and current cross sections of the reactor (g)
m_0	catalyst mass in the reactor (g)
m_c	carbon mass (g)
m_{in}	mass of an inert material in the reactor (g)
N_z	partition number along z
N_τ	partition number along τ
p_{CH_4}	partial pressure of methane (bar)
p_{H_2}	partial pressure of hydrogen (bar)
P	pressure of the gas mixture (bar)
Q	natural gas or methane consumption (l/h at standard conditions)
q	specific gas consumption (l/h g), ($=Q/m_0$)
r	dimensionless maximal specific rate of carbon formation
r_m	maximal specific rate of carbon formation (g/h g)
R	universal gas constant (J/mol K)
s	dimensionless specific carbon content
s_m	maximal dimensionless specific carbon content
s_{av}	dimensionless averaged carbon content on the catalyst
t	time (h)
t_0	time of reactor operation (h)
t_c	contact time (h)
T	temperature (K)
V	front movement rate (g/h)
x	methane conversion
x_r	equilibrium degree of methane conversion
z	dimensionless longitudinal coordinate
z_m	dimensionless reactor size

Greek letters

ε	porosity of a particle layer
ν	dimensionless rate of the front movement
ρ_c	bulk density of nanofibrous carbon (kg/m^3)
τ	dimensionless time
τ_m	dimensionless time of reactor operation
ξ	dimensionless coordinate in the reference wave system

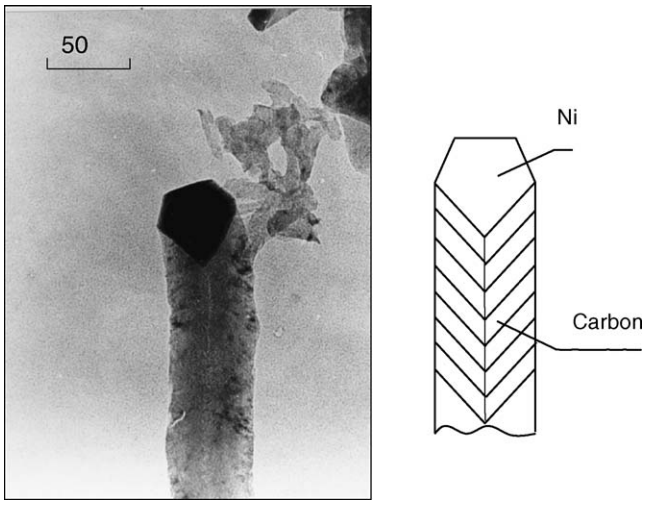

Fig. 1. Nanofibrous carbon on nickel-containing catalyst [12].

for preventing agglomeration and to intensify the heat exchange for keeping the temperature within a narrow range.

Natural gas containing predominantly methane is most abundant and inexpensive feedstock for synthesis of nanofibrous carbon, while nickel is most active to this process in comparison with the other VIII group metals. High-nickel catalysts have been developed for synthesis of NFC [21,26–29], which allow the nanofibrous carbon (carbon content up to 99.7%) to be produced from methane in the form of mesoporous granules of 1–5 mm diameter. A technology for NFC synthesis has been proposed [3,30,31] with natural and oil associated gas as feedstocks. The process of NFC synthesis from methane and natural gas is implemented on the scale of a batch fluidized bed reactor, the capacity for NFC being 0.5 kg [3] and 2.4 kg [32] during one operation cycle.

For the high-nickel catalyst (90 wt.% Ni–AlO_3) [26], the kinetics of the formation of nanofibrous carbon from a CH_4–H_2 mixture at ambient pressure has been studied [12,33] and a mathematic model including catalyst deactivation has been proposed for the observed process kinetics [34].

The industrial implementation of the process of NFC synthesis gives rise to the problem of developing calculation tools and mathematic models for the process in various reactors. The mathematic modeling of the process will make it possible not only to calculate and predict the process parameters but also to choose optimal reactor design and operation regimes.

As the first approximation, analysis of the process in reactors can be based on the commonly accepted approach in chemical technology, i.e. on the idealized model of a chemical reactor. This is a perfect-mixing reactor with respect to catalyst particles and gas. This model can be applied to laboratory shaken reactors for kinetic studies and catalyst assessment [3,12,21,27]. The analytic treatment has been done this way in Ref. [34]. The model of a plug flow reactor with a fixed catalyst bed can be used for analysis of the process in a pilot fluidized bed reactor [32] where the vibration strength is lower by an order of magnitude than in the laboratory shaken reactor, so that the particles are only prevented from agglomeration due to vibration but not mixed.

The aim of the present work is to calculate parameters of the process of NFC synthesis from methane in an isothermal plug flow reactor with a fixed catalyst bed and to identify the optimal reactor design to provide the maximal specific yield of the carbon.

2. Experimental

The calculated results given below are compared to the experimental data obtained with a pilot reactor [32] for the process of decomposition of natural gas over a high-loaded nickel catalyst. Fig. 2 is a schematic drawing of the reactor.

The reactor consisted of a top-closed stainless steel tube 1 (diameter 100 mm, height 1000 mm) with a conical bottom. There was a hole in the cone point where valve two was attached to unload the material. Gas was fed to the reaction space near the cone point through tube three arranged inside the reactor. A spiral fragment in the tube was used for pre-heating the gas. A mobile thermocouple was mounted along the reactor axis to control the temperature. The reactor was arranged inside split heater four and a heat insulator and hanged to electromagnetic vibrator five. Experimental results obtained at varied catalyst loadings are given in Table 1 where m_0 is the catalyst mass, m_{in} the mass of an inert material loaded with the catalyst, Q the natural gas consumption (l/h at standard conditions), q the specific gas consumption, $q = Q/m_0$, T temperature, m_c the produced carbon mass, G_c the specific carbon yield, $G_c = m_c/m_0$, t_0 the time of reactor operation.

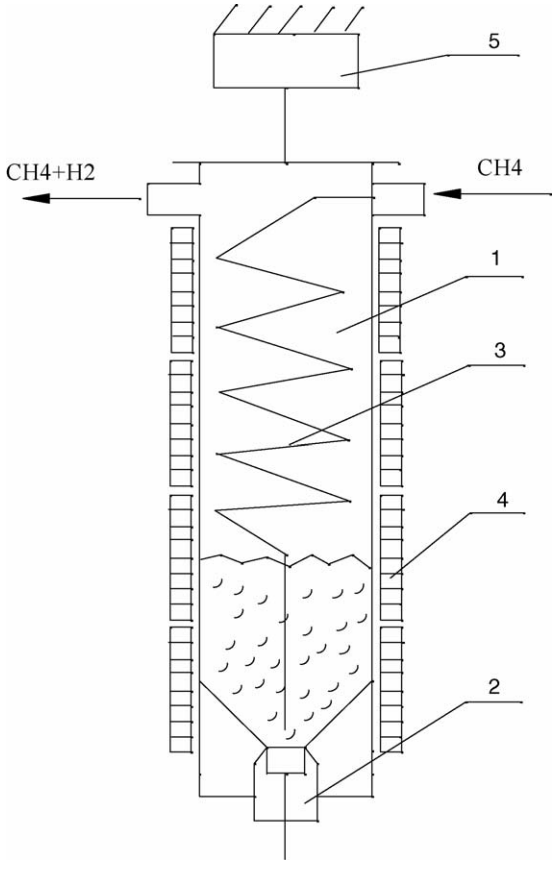

Fig. 2. Schematic diagram of pilot reactor: (1) tube, (2) unloading valve, (3) gas feeding tube, (4) heater, (5) vibrator.

Table 1
Results of testing of the pilot reactor

m_0 (g)	m_{in} (g)	Q (l/h)	q (l/h g))	T (K)	m_c (g)	G_c (g/g)	t_0 (h)
3	43	300	100	808	332	111	20
6	47	600	100	808	480	80	18
10	50	800	80	813	824	82	19
20	74	1700	85	813	1626	81	18
30	100	2000	67	803	2400	80	40

Table 2
Experimental results obtained with a vigorously shaken reactor

m_0 (g)	T (K)	q (l/h g))	G_c (g/g)
0.1	823	120	145 [21]
0.002	813	120	157 [31]

The influence of the reactor design on the specific yield of carbon was assessed using experimental data [21,31] obtained for an identical catalyst and methane in a vigorously shaken reactor where the regime close to perfect mixing of catalyst particles and gas was achieved. The data on specific carbon yield are summarized in Table 2.

3. The kinetic model of formation of nanofibrous carbon from a CH_4–H_2 mixture over a high-loaded nickel catalyst

The kinetic model of atmospheric-pressure synthesis of NFC from CH_4–H_2 mixture over a high-loaded nickel catalyst with the catalyst deactivation taken into account [34] underlies the process calculation.

In the model, the catalyst state at every instant is characterized by two parameters, the quantity of carbon formed per 1 g of catalyst c (g/g) and relative activity of the catalyst, a, ranging from 0 to 1. The catalyst deactivation is considered as a decrease in the relative catalyst activity due to carbon deposition on the catalyst surface. The catalyst is fully deactivated when the relative catalyst activity falls to zero. The following equations are proposed for the process description in time:

$$\frac{dc}{dt} = r_m a, \tag{1}$$

$$\frac{da}{dt} = -k_a r_m^2 c a, \tag{2}$$

where t is time (h) and r_m the maximal specific rate of carbon formation depending on the gas mixture composition and temperature (g/h g).

$$r_m = k\frac{p_{CH_4} - \frac{p_{H_2}^2}{K_p}}{(1 + k_H\sqrt{p_{H_2}})^2}, \tag{3}$$

pCH_4, pH_2 are partial pressures of methane and hydrogen (bar), respectively, k_a, k, K_p, k_H the coefficients depending on temper-

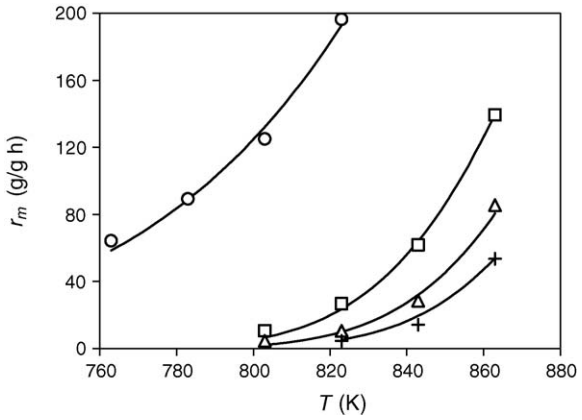

Fig. 3. Comparison of calculated data (lines) and experimental data (points) on temperature dependence of the rate of carbon formation at different hydrogen volume fractions: 0% (◯), 15% (□), 30% (△), 40% (+).

ature as

$$k_a = \exp\left(\frac{135600}{RT} - 32.077\right), \quad (4)$$

$$k = \exp\left(20.492 - \frac{104200}{RT}\right), \quad (5)$$

$$K_p = 5.088 \times 10^5 \exp\left(-\frac{91200}{RT}\right), \quad (6)$$

$$k_H = \exp\left(\frac{163200}{RT} - 22.426\right), \quad (7)$$

R is the universal gas constant (J/mol K).

The model is formulated on the basis of assessment of experimental kinetic data [12] obtained at temperature 763–863 K and hydrogen volume percentage from 0 to 40%. It is assumed that the methane decomposition into carbon and hydrogen is the limiting stage of the process:

$$CH_4 = C + 2H_2, \quad (8)$$

and abstraction of the first hydrogen atom from a methane molecule adsorbed on the catalyst surface is the limiting stage of the mechanism of reaction (8). The phenomenological approach is used for deriving the deactivation equation.

The calculated data obtained with dependence (3) and the experimental data are compared in Fig. 3. Comparative experimental and calculated data on time dependence of specific carbon yield are plotted in dimensionless coordinates in Fig. 4.

Specific features of the process kinetics are illustrated with the case when carbon is formed on the catalyst particles at constant composition of the gas medium ($pCH_4 = \text{const}$, $pH_2 = \text{const}$). When so, the carbon amount on the catalyst tends in time asymptotically to some maximal value c_m, which increases with a temperature reduction and with an increase in the hydrogen concentration in the mixture.

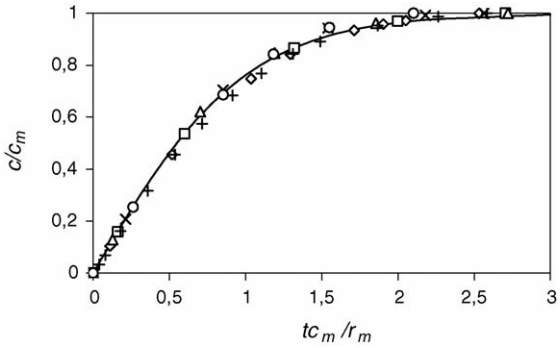

Fig. 4. Experimental (points) and calculated (lines) dependencies of dimensionless carbon content on the catalyst on dimensionless time at different temperatures and compositions of the reaction medium: 803 K 0% H_2 (◊), 823 K 0% H_2 (□), 843 K 0% H_2 (△), 863 K 0% H_2 (×), 823 K 15% H_2 (+), 843 K 15% H_2 (◯).

4. The problem formulation and derivation of equations

The isobaric-isothermal process of NFC synthesis in a plug flow reactor with a fixed catalyst bed is under consideration. Let P be the total pressure of the gas mixture and T the reactor temperature. The reactor can be represented as a tube with a catalyst of mass m_0 (g) loaded therein and methane fed thereto at the consumption Q (l/h at standard conditions). It is assumed that the process in the reactor depends only on the longitudinal coordinate but not on the transverse coordinate. Since the rate of carbon formation (3) is related to the catalyst mass, it seems suitable to choose mass, m, of the catalyst between the inlet and current cross sections of the reactor as the longitudinal coordinate. The choice of longitudinal coordinate related to the catalyst involves indirectly expansion of the catalyst bed due to formation of NFC. In the schematic of the reactor (Fig. 5), the reactor axis is drawn horizontally for convenience.

The gas mixture composition will be characterized by the methane conversion, x, with respect to pure methane. The decomposition of methane follows the pathway of reaction (8); therefore, partial pressures of methane and hydrogen relate to the methane conversion as

$$p_{CH_4}(x) = P\frac{1-x}{1+x}, \quad (9)$$

$$p_{H_2}(x) = P\frac{2x}{1+x}, \quad (10)$$

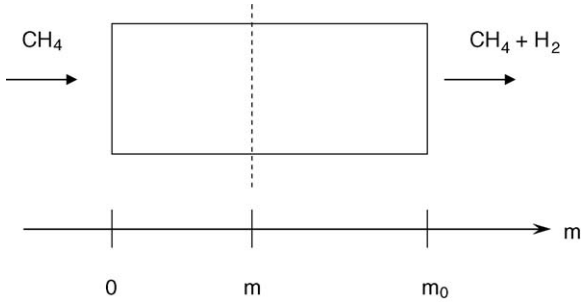

Fig. 5. Schematic drawing of reactor.

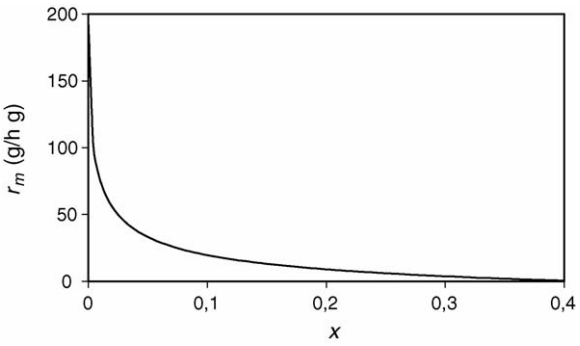

Fig. 6. Function $r_m(x)$ at $T = 823$ K and $P = 1$ bar.

with Eqs. (9) and (10), rate r_m (3) can be considered as a function of x.

$$r_m(x) = r_m(p_{CH_4}(x), \quad p_{H_2}(x)). \tag{11}$$

Function $r_m(x)$ is plotted in Fig. 6 at $T = 823$ K and $P = 1$ bar.

In the fixed catalyst bed, parameters of the catalyst (c, a) and gas (x) are functions of time t and longitudinal coordinate m.

Preceding the consideration of equations that describe the process in the reactor, we estimate the contact time of the gas in the reactor. If the characteristic parameters are $m_0 = 1$ g, $Q = 120$ l/h, $T = 823$ K, $P = 1$ bar, NFC bulk density $\rho_c = 640$ kg/m^3, porosity of a NFC particle layer $\varepsilon = 0.4$, $c_m = 150$ g/g, then the estimated contact time t_c is

$$t_c = \frac{m_0 c_m \varepsilon 273}{\rho_c Q T} = 2.6 \times 10^{-4}\,\text{h} = 0.9\,\text{s}. \tag{12}$$

The characteristic time of the catalyst deactivation under given conditions is several hours or dozens hours [12,21,32], i.e. longer than the contact time by several orders of magnitude. Hence, it is reasonable to conclude that a quasistationary approximation is valid for the gas phase, and the gas characteristics obey the stationary equations related to the catalyst state at the instant under consideration.

Let the value J_c (g/h) be the flux of carbon, which enters the reactor as a component of inlet methane.

$$J_c = \frac{Q12}{22.4}, \tag{13}$$

where 12 g/mol is the molecular mass of carbon, 22.4 l/mol the volume of 1 mol of gas at standard conditions.

Then the equation set describing dynamics of the processes of carbon deposition and catalyst deactivation in the reactor will be

$$\frac{\partial c}{\partial t} = r_m(x)a, \tag{14}$$

$$\frac{\partial a}{\partial t} = -k_a r_m^2(x) c a, \tag{15}$$

$$J_c \frac{\partial x}{\partial m} = r_m(x)a. \tag{16}$$

Eqs. (14) and (15) correspond to kinetic Eqs. (1) and (2), and Eq. (16) is derived by inspecting the carbon balance over the reactor at quasistationary approximation.

The equation set (14)–(16) needs to be added with initial and boundary conditions for functions $c(t,m)$, $a(t,m)$ and $x(t,m)$

$$c(0,\ m) = 0, \quad a(0, m) = 1, \quad x(t,\ 0) = 0. \tag{17}$$

To simplify the equations and calculations, dimensionless values are introduced:

$$r(x) = \frac{r_m(x)}{r_m(0)}, \tag{18}$$

$$s = \sqrt{k_a r_m(0)}c, \tag{19}$$

$$\tau = r_m(0)\sqrt{k_a r_m(0)}t, \tag{20}$$

$$z = \frac{r_m(0)}{J_c}m. \tag{21}$$

With the new variables, the equations, the initial and boundary conditions (14)–(17) change to

$$\frac{\partial s}{\partial \tau} = r(x)a, \tag{22}$$

$$\frac{\partial a}{\partial \tau} = -r^2(x)sa, \tag{23}$$

$$\frac{\partial x}{\partial z} = r(x)a, \tag{24}$$

$$s(0, z) = 0, \quad a(0, z) = 1, \quad x(\tau, 0) = 0. \tag{25}$$

5. Solution in the form of progressive wave of the catalyst deactivation

In kinetic studies, the lower hydrogen concentration, the faster is the catalyst deactivation process. Hence, the catalyst layers nearby the inlet section of the reactor will be faster deactivated than the farther layers. As a result, a transition region appears between the deactivated and maximally active catalyst layers which transfers along the direction of gas flowing. If a reactor with a rather large catalyst loading is under consideration, questions arise naturally, if profiles s, a and x are stabilized and if there is a solution in the form of a wave moving at a constant rate and possessing its stationary profile.

To answer the question, we shall search for the solution in the form of progressive wave for equation set (22)–(24):

$$s(\tau, z) = s(\xi), \quad a(\tau, z) = a(\xi), \quad x(\tau, z) = x(\xi), \tag{26}$$

where $\xi = z - v\tau$, and v the dimensionless rate of the front movement.

Substituting (26) in (22)–(24), we get

$$-v\frac{ds}{d\xi} = r(x)a, \tag{27}$$

$$-v\frac{da}{d\xi} = -r^2(x)sa, \tag{28}$$

$$\frac{dx}{d\xi} = r(x)a. \tag{29}$$

At $\xi = -\infty$, the boundary conditions will be: the catalyst is fully carbonized and deactivated, the gas is methane

$$s(-\infty) = s_m, \quad a(-\infty) = 0, \quad x(-\infty) = 0, \tag{30}$$

where s_m is the dimensionless carbon amount on the deactivated catalyst (this is as yet unknown value). At $\xi = \infty$: the catalyst is free of carbon and reveals the maximal activity, the gas is an equilibrium mixture of methane and hydrogen

$$s(\infty) = 0, \quad a(\infty) = 1, \quad x(\infty) = x_r, \tag{31}$$

where x_r is the calculated equilibrium degree of methane conversion in the given process at the condition of $r(x_r) = 0$.

It follows from Eqs. (27) and (29) that

$$v\frac{ds}{d\xi} + \frac{dx}{d\xi} = 0. \tag{32}$$

Integrating (32) with boundary conditions (30) and (31) gives

$$vs + x = \text{const} = vs_m = x_r. \tag{33}$$

It follows from Eq. (33) that

$$s = \frac{x_r - x}{v}, \tag{34}$$

$$s_m = \frac{x_r}{v}. \tag{35}$$

Substituting Eq. (34) into Eq. (28) and combining the latter with Eq. (29), we have an equation set for a and x:

$$\frac{da}{d\xi} = \frac{1}{v^2} r^2(x)(x_r - x)a, \tag{36}$$

$$\frac{dx}{d\xi} = r(x)a. \tag{37}$$

With eliminated ξ, from Eqs. (36) and (37) follows the equation

$$v^2 da = r(x)(x_r - x)dx, \tag{38}$$

which can be integrated with allowance for Eq. (30) to give the relationship between a and x:

$$v^2 a = \int_0^x r(x)(x_r - x)dx. \tag{39}$$

With $\xi = \infty$ and boundary condition (31), we can derive from Eq. (39) the formula for calculating the front movement rate:

$$v = \sqrt{\int_0^{x_r} r(x)(x_r - x)dx}. \tag{40}$$

Finally, s_m is determined from Eq. (35), and profiles a and x can be calculated by solving numerically the equation set (36) and (37). For example, the Runge-Kutta method can be applied with $x = x_r/2$ taken as the reference point ($\xi = 0$) and the initial condition for a determined from Eq. (39).

The calculation is done at $T = 823$ K and $P = 1$ bar. From the calculation, $x_r = 0.41$, $v = 0.104$, $s_m = 4.0$. At $Q = 120$ l/h, the dimensional values are: front movement rate $V = J_c\sqrt{k_a r_m(0)}v = 0.2$ g/h, maximal specific carbon content $c_m = s_m/\sqrt{k_a r_m(0)} = 132$ g/g. Note for the dimensional values, the maximal specific carbon content c_m is independent of the consumption of the gas mixture and the front rate V is proportional to J_c.

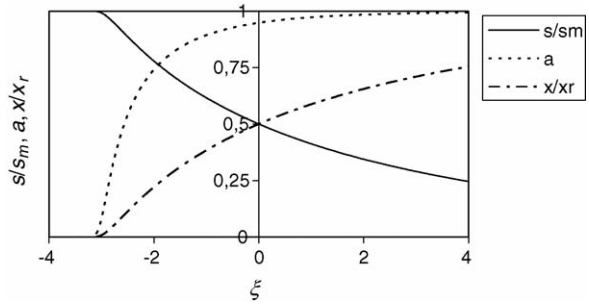

Fig. 7. Profiles s/s_m, a and x/x_r vs. ξ at $T = 823$ K.

Profiles of dimensionless values $s(\xi)/s_m$, $a(\xi)$, $x(\xi)/x_r$ are shown in Fig. 7.

6. Calculation of the process for a reactor with finite catalyst loading

The calculation is aimed at determination of values $s(\tau, z)$, $a(\tau, z)$ and $x(\tau, z)$ to fit Eqs. (22)–(24) and conditions (25) in a certain region $0 \le z \le z_m$ and $0 \le \tau \le \tau_m$, where z_m and τ_m are the region boundaries.

Equation set (22)–(24) is a hyperbolic type system with characteristics $z = \text{const}$ and $\tau = \text{const}$. For the calculation, a grid is constructed along z and τ with nodes in the points

$$z_j = j \cdot h_z \qquad j = 0 \ldots N_z, \tag{41}$$

$$\tau_i = i \cdot h_\tau \qquad i = 0 \ldots N_\tau, \tag{42}$$

where h_z, h_τ, N_z, N_τ are steps of grid and partition numbers along z and τ, respectively.

The first unknown values to calculate are s, a and x at the region boundaries $\tau = 0$ and $z = 0$.

The value for x at the boundary $\tau = 0$ is determined by Eq. (24). Taking into consideration $a = 1$, the equation is written in the form

$$\frac{\partial x}{\partial z} = r(x). \tag{43}$$

Eq. (43) with the initial conditions $x(0, 0) = 0$ is numerically solved by the constant step Runge-Kutta method.

At the boundary $z = 0$, the values for s and a are calculated using the equation set (22) and (23). Taking into account that $x = 0$ at this boundary, the equations are given by

$$\frac{\partial s}{\partial \tau} = a, \tag{44}$$

$$\frac{\partial a}{\partial \tau} = -sa. \tag{45}$$

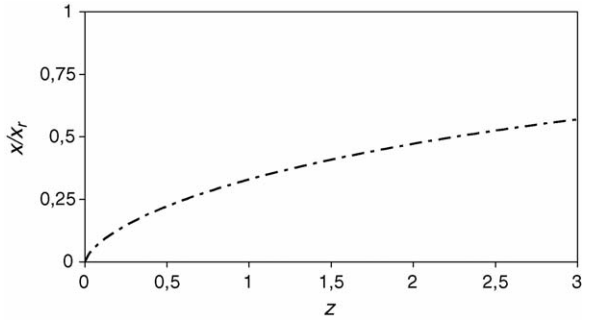

Fig. 8. Profile s/s_m vs. z at $\tau = 0$.

The equation set (22) and (23) with the boundary conditions $s(0, 0) = 0$ and $a(0, 0) = 1$ has an analytical solution

$$s(\tau, 0) = \sqrt{2} th\left(\frac{\tau}{\sqrt{2}}\right), \quad (46)$$

$$a(\tau, 0) = \frac{1}{ch^2\left(\frac{\tau}{\sqrt{2}}\right)}. \quad (47)$$

Within the region of $0 < z \leq z_m$, $0 < \leq \tau_m$, the values for s, a and x are calculated by the method of characteristics [35].

The following initial parameters are used for the calculations: catalyst loading $m_0 = 1$ g in the reactor, temperature $T = 823$ K, pressure $P = 1$ bar, methane consumption $Q = 120$ l/h, and operation time of the reactor is ca. 10 h. Note that the process in the reactor is determined in fact by two parameters: temperature and, according to Eq. (21), specific consumption of methane Q/m_0. The preset parameters are relevant to the region with boundaries at $z_m = 3.0$ and $\tau_m = 60$. $N_z = 100$ and $N_\tau = 200$ are chosen for the calculations.

The calculated results are illustrated in Figs. 8–12, where profiles s/s_m, a and x/x_r versus z are plotted in dimensionless coordinates for different instants τ; here s_m is the maximal carbon content in the reactor with an infinite catalyst loading ($s_m = 4.0$), x_r the equilibrium degree of methane conversion at 823 K ($x_r = 0.41$).

Fig. 8 ($\tau = 0$) shows an only profile of x/x_r since $s = 0$ and $a = 0$. Fig. 12 ($\tau = 60$) shows an only profile of s/s_m since $a = 0$ and $x = 0$.

One can see that a deactivation wave propagates along the reactor. Until all the catalyst is active, s falls monotonically along the reactor. After the deactivated catalyst region has appeared, the profile of s has a maximum at the front boundary, the profile being not any longer varied in time behind the front. After all the catalyst has been deactivated, s increases as goes away from the inlet.

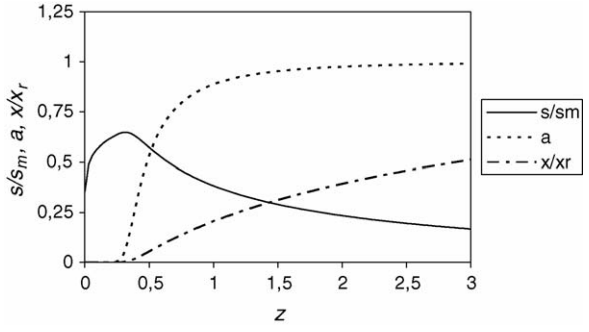

Fig. 9. Profiles s/s_m, a and x/x_r vs. z at $\tau = 18$.

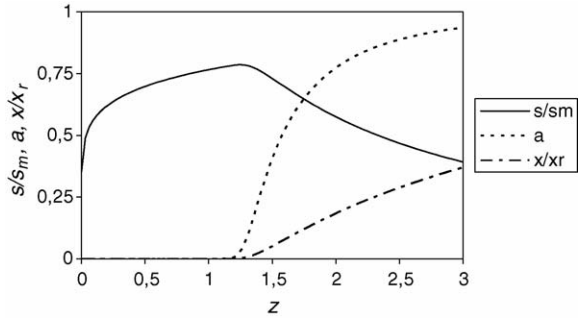

Fig. 10. Profiles s/s_m, a and x/x_r vs. z at $\tau = 36$.

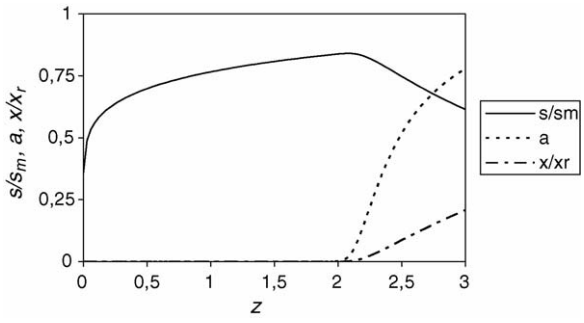

Fig. 11. Profiles s/s_m, a and x/x_r vs. z at $\tau = 48$.

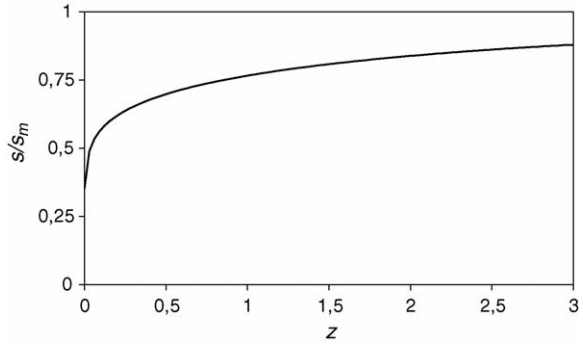

Fig. 12. Profile s/s_m vs. z at $\tau = 60$.

From the calculations, the reactor length averaged content of carbon on the catalyst (after the catalyst deactivation) is $s_{av} = 3.125$ or, in dimensional form, $G_c = c_{av} = 103$ g/g.

7. Discussion

According to the calculations [34], at identical conditions (temperature 823 K, specific consumption of methane 120 l/h g) the specific yield of carbon is 159 g/g in the reactor with perfect gas and catalyst particles mixing, i.e. 1.6 times as high as that

in the fixed catalyst bed reactor. The reasons may be as follows. Kinetic studies of the process of carbon formation from methane reveal a common feature: The higher carbon formation rate, the faster is the catalyst deactivation and the lower specific carbon yield. It is known that when the chemical reaction rate increases with an increase in a reactant concentration, the average reaction rate is higher in a plug flow reactor than in a perfect mixing reactor at otherwise identical conditions [36]. In the process under consideration, the reaction rate is proportional to the concentration of methane. Hence, the average rate is higher in a plug flow reactor than in a perfect mixing reactor; as a result, the catalyst is faster deactivated but the specific carbon yield is lower in the plug flow reactor.

There may be another explanation. As the hydrogen partial pressure increases in the mixture, the catalyst deactivation rate decreases and the specific carbon yield increases. In an ideal mixing reactor the catalyst is entirely in the methane-hydrogen medium. In a plug-flow reactor, a part of the catalyst (at the boundary of the deactivation front) undergoes carbonization in the pure methane medium that results in an accelerated catalyst deactivation and in a decrease in the specific carbon yield.

The modeling results also elucidate why the specific carbon yield is lower in the pilot reactor [32] than in the laboratory fluidized bed reactor [21,31]. The operation regime in the laboratory fluidized bed reactor is close to perfect mixing of catalyst particles and gas, and the specific carbon yield reaches ca. 150 g/g. The pilot facility operates for most time in the fixed bed regime, the specific carbon yield being ca. 80 g/g. Thus, the specific yield decreases by a factor of 1.9. The calculations predict a qualitatively similar picture but the predicted decrease in the specific yield is less than that observed in practice. Some divergence between the calculated and observed data can be accounted for by that the experimental data are obtained using a quartz reactor and pure methane, while the pilot reactor is made of stainless steel and tested with natural gas containing impurities.

8. Conclusions

Under consideration was the process of synthesis of nanofibrous carbon from methane achieved in an isothermal plug flow reactor with a fixed bed of catalyst 90 wt.% Ni–Al_2O_3. It was shown that the equations allow a solution in the form of progressive wave of deactivation that moves at a constant rate and has a stationary profile. Analytic dependencies were obtained to calculate the wave rate and carbon content in the deactivated catalyst. The process calculation was performed for a reactor at 823 K and specific methane consumption 120 l/h g. The process parameters for the plug flow reactor with the fixed catalyst bed were compared to those for the reactor with perfect mixing of catalyst particles and gas, both operating at identical conditions. It was shown that the specific carbon yield is higher in the latter than in the former. The mathematic modeling results are in good qualitative agreement with the experimentally observed decrease in the specific carbon yield in the pilot reactor in comparison to that in the laboratory fixed bed reactor.

Acknowledgements

The present work was supported by the Scientific and Engineering Program “Scientific studies of Higher School on Priority Areas of Science and Engineering” (Grant 203.06.03.001) and the Russian Foundation for Basic Research (Grant 04-03-32618).

References

[1] R.T.K. Baker, P.S. Harris, in: P.L. Walker, P.A. Thrower (Eds.), Chemistry and Physics of Carbon, vol. 14, Marcel Dekker, New York, 1978, p. 83.
[2] N.M. Rodrigues, J. Mater. Res. 8 (1993) 3233.
[3] G.G. Kuvshinov, L.B. Avdeeva, O.V. Goncharova, Yu.I. Mogilnykh, Extended abstracts international meeting on chemical engineering and biotechnology, in: Thermal Process Engineering, ACHEMA‘94, Frankfurt on Main, 5–11 June, 1994, p. 96.
[4] V.V. Chesnokov, R.A. Buyanov, Russ. Chem. Rev. 69 (2000) 623.
[5] V.K. Frantsuzov, A.P. Petrusenko, B.V. Peshnev, A.L. Lapidus, Khim. Tverd. Topl. (Moscow) 2 (2000) 52.
[6] K.P. Jong, J.W. Geus, Catal. Rev. Sci. Eng. 42 (2000) 481.
[7] V.B. Fenelonov, L.B. Avdeeva, V.I. Zheivot, L.G. Okkel, O.V. Goncharova, L.G. Pimneva, Kinet. Catal. 34 (1993) 483.
[8] G.G. Kuvshinov, Yu.I. Mogilnykh, M.Yu. Lebedev, American Chemical Society, Division of Fuel Chemistry 43 (4) (1998) 846.
[9] N.M. Rodrigues, M.S. Kim, R.T.K. Baker, J. Phys. Chem. 98 (1994) 13108.
[10] J.-M. Nhut, L. Pesant, J.-P. Tessonnier, G. Wine, J. Guille, C. Pham-Huu, M.-J. Ledoux, Appl. Catal. A 254 (2003) 345.
[11] G.A. Kovalenko, E.V. Kuznetsova, Yu.I. Mogilnykh, I.S. Andreeva, D.G. Kuvshinov, N.A. Rudina, Carbon 39 (2001) 1033.
[12] G.G. Kuvshinov, Yu.I. Mogilnykh, D.G. Kuvshinov, V.I. Zaikovskii, L.B. Avdeeva, Carbon 36 (1998) 87.
[13] M.C. Demicheli, E.N. Pouzi, A.O. Ferretti, A.A. Yeramian, Chem. Eng. J. 46 (1991) 129.
[14] J.-W. Snoeck, G.F. Froment, M. Fowles, J. Catal. 169 (1997) 250.
[15] E.G.M. Kuijpers, J.W. Jansen, A.J. van Dillen, J.W. Geus, J. Catal. 72 (1981) 75.
[16] P. Chen, H.-B. Zhang, G.-D. Lin, Q. Hong, K.R. Tsai, Carbon 35 (1997) 1495.
[17] T. Zhang, M.D. Amiridis, Appl. Catal. A 167 (1998) 161.
[18] T.V. Choudhary, C. Sivadinarayana, C.C. Chusuei, A. Klinghoffer, D.W. Goodman, J. Catal. 199 (2001) 9.
[19] V.R. Choudhary, S. Banerjee, A.M. Rajput, Appl. Catal. A 234 (2002) 259.
[20] E. Couteau, K. Hernadi, J.W. Seo, L. Thien-Nga, Cs. Miko, R. Gaal, L. Forro, Chem. Phys. Lett. 378 (2003) 9.
[21] L.B. Avdeeva, O.V. Goncharova, D.I. Kochubey, V.I. Zaikovskii, L.M. Plyasova, B.N. Novgorodov, Sh.K. Shaikhutdinov, Appl. Catal. A 141 (1996) 117.
[22] E.R. Gilliland, P. Harriott, Ind. Eng. Chem. 46 (1954) 2195.
[23] G.G. Kuvshinov, Yu.I. Mogilnykh, D.G. Kuvshinov, S.G. Zavarukhin, V.N. Parmon, Proceeding of the 11th World Hydrogen Energy Conference, Stuttgart, Germany, 23–28 June, 1996, p. 655.
[24] A. Steinfeld, V. Kirillov, G. Kuvshinov, Y. Mogilnykh, A. Reller, Chem. Eng. Sci. 52 (1997) 3599.
[25] Y. Wang, F. Wei, G. Luo, H. Yu, G. Gu, Chem. Phys. Lett. 364 (2002) 568.
[26] O.V. Goncharova, L.B. Avdeeva, V.B. Fenelonov, L.M. Plyasova, V.V. Malakhov, G.S. Litvak, A.A. Vlasov, Kinet. Catal. 36 (1995) 268.
[27] M.A. Ermakova, D.Yu. Ermakov, G.G. Kuvshinov, L.M. Plyasova, J. Catal. 187 (1999) 77.
[28] M.A. Ermakova, D.Yu. Ermakov, G.G. Kuvshinov, Appl. Catal. A 201 (2000) 61.

[29] G.G. Kuvshinov, Yu.I. Mogilnykh, D.G. Kuvshinov, D.Yu. Yermakov, M.A. Yermakova, A.N. Salanov, N.A. Rudina, Carbon 37 (1999) 1239.
[30] G.G. Kuvshinov, Proceedings of the Third International Conference on new Energy Systems and Conversions, Kazan (Russia), 1997, p. 47.
[31] D.G. Kuvshinov, Development of the Process for Catalytic Processing of Hydrocarbon Gases to Produce Filamentous Carbon and Hydrogen, PhD Thesis, Boreskov Institute of Catalysis, Novosibirsk, 2000.
[32] G.G. Kuvshinov, S.G. Zavarukhin, Yu.I. Mogilnykh, D.G. Kuvshinov, Russian Chemical Industry 5 (1998) 300.
[33] G.G. Kuvshinov, Yu.I. Mogilnykh, D.G. Kuvshinov, Catal. Today 42 (1998) 357.
[34] S.G. Zavarukhin, G.G. Kuvshinov, Appl. Catal. A 272 (2004) 219.
[35] G.N. Lance, Numerical Methods for High Speed Computers, Iliffe and Sons LTD, London, 1960.
[36] G.F. Froment, K.B. Bischoff, Chemical reactor analysis and design, Wiley, New York a.o, 1979.